Optical and Quantum Electronics **34:** 1191–1200, 2002.

Comparison of 1300 nm quantum well lasers using different material systems

G. LIN* AND C.P. LEE
Department of Electronics Engineering, National Chiao Tung University, Hsinchu, Taiwan, Republic of China
*(*author for correspondence: E-mail: graylin@itri.org.tw)*

Abstract. The band structure and material gain are calculated for 1300-nm band quantum well lasers of GaInNAs, AlGaInAs and GaInAsP material systems. The material compositions for each system are carefully chosen for comparison. The calculated results show that the peak gain is around the same in spite of the difference in band structures for the three systems.

Key words: band offset ratio, band structure, material gain, 1300-nm band, quaternary material system

1. Introduction

The optical communications market has seen a great expansion due to the strong demand for subscriber-loop applications such as fiber-in-the-loop (FITL) and fiber-to-the-home (FTTH). 1300-nm band quantum well lasers are the key components in these optical fiber communication systems. The emitters should be temperature insensitive for uncooled system and low-cost for common subscribers. Nevertheless, the GaInAsP system on InP substrate suffers from poor temperature characteristics due to electron overflow over the rather small conduction band offset. Although AlGaInAs system has been proposed for better high-temperature operation, the theoretical and experimental comparison does not seem to be based on the same basis.

Recently, GaInNAs system on GaAs substrates has been successfully demonstrated for 1300 nm lasers. The large band gap bowing makes the long-wavelength lasing possible for devices made with such material system based on low-cost GaAs substrates. The huge conduction band offset also contributes to the superior high-temperature characteristics (Kondow *et al.* 1997).

In this paper, we present theoretical comparison for the quantum well lasers based on GaInAsP, AlGaInAs and GaInNAs systems emitting at 1300 nm. The material parameters and the relevant models for different material systems are described. The criterion for choosing the material

composition is also given. Finally, the material gain is calculated and compared. In this way the lasers are compared in the equal footing.

2. Theoretical background

2.1. BAND STRUCTURE CALCULATION

The valence band structure ($E_v - k_t$) is calculated by using the block-diagonalized 3×3 strained Luttinger–Kohn Hamiltonian (Chuang 1995) and is given by

$$H_{3\times3}^{U,L} = -\begin{bmatrix} P+Q & |R_k| \mp \mathrm{i}|S_k| & \sqrt{2}|R_k| \pm \frac{\mathrm{i}}{\sqrt{2}}|S_k| \\ |R_k| \pm \mathrm{i}|S_k| & P-Q & \sqrt{2}Q \pm \mathrm{i}\sqrt{\frac{3}{2}}|S_k| \\ \sqrt{2}|R_k| \mp \frac{\mathrm{i}}{\sqrt{2}}|S_k| & \sqrt{2}Q \mp \mathrm{i}\sqrt{\frac{3}{2}}|S_k| & P+\Delta \end{bmatrix} + V_v \quad (1)$$

where

$$\begin{aligned} &P = P_k + P_\varepsilon \quad Q = Q_k + Q_\varepsilon \\ &P_k = \frac{\hbar^2}{2m_0}\left(\gamma_1 k_t^2 - \frac{\partial}{\partial z}\gamma_1\frac{\partial}{\partial z}\right) \quad Q_k = \frac{\hbar^2}{2m_0}\left(\gamma_2 k_t^2 + 2\frac{\partial}{\partial z}\gamma_2\frac{\partial}{\partial z}\right) \\ &|R_k| \approx \frac{\hbar^2}{2m_0}\frac{\sqrt{3}}{2}(\gamma_2+\gamma_3)k_t^2 \quad |S_k| = -\mathrm{i}\frac{\hbar^2}{2m_0}\sqrt{3}k_t\left(\frac{\partial}{\partial z}\gamma_3 + \gamma_3\frac{\partial}{\partial z}\right) \\ &P_\varepsilon = -a_v(\varepsilon_{xx}+\varepsilon_{yy}+\varepsilon_{zz}) \quad Q_\varepsilon = -\frac{b}{2}(\varepsilon_{xx}+\varepsilon_{yy}-2\varepsilon_{zz}) \\ &\varepsilon_{xx} = \varepsilon_{yy} = \frac{a_0-a}{a} \quad \varepsilon_{zz} = -\frac{2C_{12}}{C_{11}}\varepsilon_{xx} \quad \varepsilon_{xy} = \varepsilon_{yz} = \varepsilon_{zx} = 0 \end{aligned} \quad (2)$$

Here, the strain components, ε_{xx}, ε_{yy}, and ε_{zz}, are related to the lattice constant of the active layer and the substrate (a and a_0, respectively), and the elastic constant C_{11} and C_{12}. For calculating the conduction band structure, the single-band effective mass equation is used. With strain included, the Hamiltonian is given by

$$H_c = \frac{\hbar^2}{2}\left(\frac{k_t^2}{m_{ct}} - \frac{\partial}{\partial z}\frac{1}{m_{cz}}\frac{\partial}{\partial z}\right) + V_c + a_c(\varepsilon_{xx}+\varepsilon_{yy}+\varepsilon_{zz}) \quad (3)$$

The band offset, V_v in Equation (1) and V_c in Equation (3), will be treated in the following subsection.

2.2. CALCULATION OF STRAINED BULK BAND GAP

Setting the unstrained valence band-edge of the active region material as the reference energy of zero. The strained bulk valence band-edge, determined from Equation (1) with $k = 0$, is shifted by

$$\begin{aligned} \delta E_{hh} &= -P_\varepsilon - Q_\varepsilon \quad \text{(compressive)} \\ \delta E_{lh} &= -P_\varepsilon + Q_\varepsilon \quad \text{(tensile)} \end{aligned} \tag{4}$$

and the strained bulk conduction band-edge, determined from Equation (3) with $k = 0$, is shifted by

$$\delta E_c = a_c(\varepsilon_{xx} + \varepsilon_{yy} + \varepsilon_{zz}) \tag{5}$$

The strained band gap, E_{gs}, can therefore be expressed as

$$E_{gs} = \begin{cases} E_{gu} + \delta E_c - \delta E_{hh} & \text{(compressive)} \\ E_{gu} + \delta E_c - \delta E_{lh} & \text{(tensile)} \end{cases} \tag{6}$$

2.3. CALCULATION OF BAND OFFSET

The relative band alignment of band-edges between the quantum well and the barrier is very important, nevertheless controversial, for modeling semiconductor quantum well structures. This is rather complicated for the strained case. Two models regarding the band alignment are reviewed and chosen for the relevant quaternary systems.

(1) Model-solid theory (Van der Walle 1989): The valence band position is given by

$$E_v = \begin{cases} E_{v,av} + \frac{\Delta}{3} + \delta E_{hh} & \text{for hh} \\ E_{v,av} + \frac{\Delta}{3} + \delta E_{lh} & \text{for lh} \end{cases} \tag{7}$$

where $E_{v,av}$ is the average valence band-edge energy and Δ is the spin-orbit split-off energy. The conduction band position can be calculated by simply adding the strained band gap energy, E_{gs}, to the valence band position. The conduction band offset ratio is given by

$$\frac{\Delta E_c}{\Delta E_g} = 1 - \frac{E_v^w - E_v^b}{E_{gs}^b - E_{gs}^w} \tag{8}$$

where E_{gs}^{w} and E_{gs}^{b} are the strained band gaps for the well and the barrier, respectively.
(2) Harrison's model (Harrison 1977): The band-edge positions of the conduction band and the valence band are given by

$$\begin{aligned} E_{v}^{H} &= \begin{cases} E_{vH} + \delta E_{hh} & \text{for hh} \\ E_{vH} + \delta E_{lh} & \text{for lh} \end{cases} \\ E_{c}^{H} &= E_{cH} + \delta E_{c} \end{aligned} \tag{9}$$

where E_{vH} and E_{cH} are Harrison's band-edge energy. The conduction band offset ratio is then given by

$$\frac{\Delta E_{c}}{\Delta E_{g}} = \frac{E_{c}^{H,b} - E_{c}^{H,w}}{(E_{c}^{H,b} - E_{c}^{H,w}) + (E_{v}^{H,w} - E_{v}^{H,b})} \tag{10}$$

where the superscript 'w' and 'b' refer to the well and the barrier, respectively.

2.4. CALCULATION OF MATERIAL GAIN

The optical gain is calculated based on the Fermi's Golden Rule and Lorentzian lineshape function with an intraband relaxation time of 0.1 ps. Only TE modal gain is calculated for compressive strain that we are concerned here. The momentum matrix elements for the quaternary active layer are interpolated from their binary constituents. The material and band parameters used in the calculation are listed in Table 1.

3. Simulation details

Unless otherwise specified, the material parameters P for quaternary GaInAsP, AlGaInAs and GaInNAs systems are interpolated from their respective binary or ternary constituents and are given as,

$$\begin{aligned} P(\mathrm{Ga}_x\mathrm{In}_{1-x}\mathrm{As}_y\mathrm{P}_{1-y}) &= xy\mathrm{P}(\mathrm{GaAs}) + (1-x)(1-y)\mathrm{P}(\mathrm{InP}) \\ &\quad + (1-x)yP(\mathrm{InAs}) + x(1-y)P(\mathrm{GaP}) \\ P(\mathrm{Ga}_x\mathrm{Al}_y\mathrm{In}_{1-x-y}\mathrm{As}) &= xP(\mathrm{GaAs}) + yP(\mathrm{AlAs}) + (1-x-y)P(\mathrm{InAs}) \\ P(\mathrm{Ga}_x\mathrm{In}_{1-x}\mathrm{N}_y\mathrm{As}_{1-y}) &= P(\mathrm{Ga}_x\mathrm{In}_{1-x}\mathrm{As}) + P(\mathrm{GaN}_y\mathrm{As}_{1-y}) - P(\mathrm{GaAs}) \end{aligned} \tag{11}$$

The material parameters of the binary semiconductors are listed in Table 1. For GaInNAs system, the material parameters of GaInAs is used because the N content is rather small ($\sim$1%) in quantum well lasers.

Table 1. Material parameters for the calculation for GaInAsP and AlGaInAs and GaInNAs material systems

Materials	GaAs	AlAs	InAs	InP	GaP	GaN
Parameters						
a_0 (Å)	5.6533	5.6600	6.0584	5.8688	5.4505	4.503
E_g (eV) at RT	1.424	3.03	0.354	1.344	2.78	3.40
Δ (eV)	0.34	0.28	0.38	0.11	0.08	–
MME (eV)	25.7	21.1	22.2	20.7	22.2	–
Deformation potential (eV)						
a_c (eV)	−7.17	−5.64	−5.08	−5.04	−7.14	–
a_v (eV)	1.16	2.47	1.00	1.27	1.70	–
b (eV)	−1.7	−1.5	−1.8	−1.7	−1.8	–
C_{11} (10^{11} dyne/cm^2)	11.879	12.5	8.329	10.11	14.05	–
C_{12} (10^{11} dyne/cm^2)	5.376	5.34	4.526	5.61	6.203	–
Effective mass (in unit of $\hbar^2/2m_0$)						
γ_1	6.8	3.45	20.4	4.95	4.05	–
γ_2	1.9	0.68	8.3	1.65	0.49	–
γ_3	2.73	1.29	9.1	2.35	1.25	–
Model-solid theory (average valence-band-edge energy)						
$E_{v,av}$ (eV)	–6.92	–7.49	–6.67	–7.04	–7.40	–
Harrison's Model (valence-band-edge energy in reference scale)						
E_{vH} (eV)	0.111	–0.4245	0.441	0	–0.388	–
E_{cH} (eV)	1.531	2.5255	0.801	1.35	2.352	–

One exception to above interpolation formula is the unstrained band gap. For GaInAsP, AlGaInAs systems, and GaInAs/GaNAs in the GaInNAs system, the unstrained band gap is given as,

$$\begin{aligned}
E_{gu}(Ga_xIn_{1-x}As_yP_{1-y}) &= 1.35 + 0.668x - 1.068y + 0.758x^2 + 0.078y^2 \\
&\quad - 0.069xy - 0.322x^2y + 0.03xy^2(\text{eV}) \\
E_{gu}(Al_xGa_yIn_{1-x-y}As) &= 0.36 + 2.093x + 0.629y + 0.577x^2 + 0.436y^2 \\
&\quad + 1.013xy - 2.0xy(1-x-y)(\text{eV}) \\
E_{gu}(Ga_xIn_{1-x}As) &= 0.36 + 0.509x + 0.555x^2(\text{eV}) \\
E_{gu}(GaN_yAs_{1-y}) &= 1.424 - 14.024y + 18y^2(\text{eV})
\end{aligned} \tag{12}$$

All the band gap data are taken from (Chuang 1995) except that for ternary GaNAs which is taken from (Takeuchi *et al.* 1998).

Regarding to the band offsets, different model is chosen for different material systems. For GaInAsP and AlGaInAs systems on InP substrate, Harrison's model, instead of model-solid theory, is used because it has a better agreement with the empirical results (Minch *et al.* 1999). For the GaInNAs system on GaAs substrate, the model-solid theory is used as in the case for strained GaInAs materials.

As a first-order approximation, we use the momentum matrix element of GaInAs for the GaInNAs system. However, due to the interaction between the conduction band and the nitrogen states, a more accurate calculation should include a correction factor, $f_{\Gamma c}$ (Lindsay and O'Reilly 1999).

4. Results

Fig. 1 shows the contour plot relating x and y to the strain and the strained bulk band gap of $Ga_xIn_{1-x}As_yP$, $Ga_xAl_yIn_{1-x-y}As$, and $Ga_xIn_{1-x}N_yAs_{1-y}$ systems. The solid lines are for strained bulk band gap and the short-dashed lines are for strain. The long-dashed line delimits the boundary between type-I and type-II heterojunctions. For lasing transition in 1300-nm band, we choose the strained bulk band gap around 0.9 eV in account of quantum confinement of 0.05 eV.

The conduction band offset ratio versus Ga composition for GaInAsP and AlGaInAs systems on InP are shown in Fig. 2. The solid line and dashed line are for the latticed-matched GaInAsP and AlGaInAs systems, respectively, while the enclosed regions are for strained systems with strained bulk band gap of 0.9 ± 0.02 eV. It reveals that the conduction band offset is larger for lower Ga content or higher compressive strain. So, to increase the conduction band offset can be achieved by maximizing the compressive strain (or minimizing the Ga content). The quaternary compositions for GaInAsP and AlGaInAs are therefore determined for subsequent band structure calculation. For the GaInNAs system, the N content and the maximum allowable compressive strain should be practical otherwise the device performance may degrade. The quaternary compositions chosen for the active layers for these material systems are marked by 'X' in Fig. 1.

Fig. 3 shows calculated band structure for different material system combinations. The zero energy is chosen to be the top of the unstrained valence band. The strained band-edge and the barrier band-edge are also determined and shown in the figure for comparison. The lowest transition wavelength is around 1300 nm. The well width chosen is 70 Å for all the material combinations and the value of the compressive strain chosen is for practical consideration. The barrier band gap wavelength is 1100 nm for both GaInAsP and AlGaInAs on InP substrates, while the barrier band gap for the GaInNAs lasers is that of GaAs. The strained band offset ratio (ΔE_c:ΔE_v) for the three material combinations, InAsP/GaInAsP, AlInAs/AlGaInAs and GaInNAs/GaAs, are 0.48:0.52, 0.51:0.49 and 0.74:0.26, respectively. For InAsP/AlGaInAs, the strained band offset ration is 0.70:0.30. In terms of larger conduction band discontinuity, it is the best choice to have GaInAsP over AlGaInAs on InP substrate.

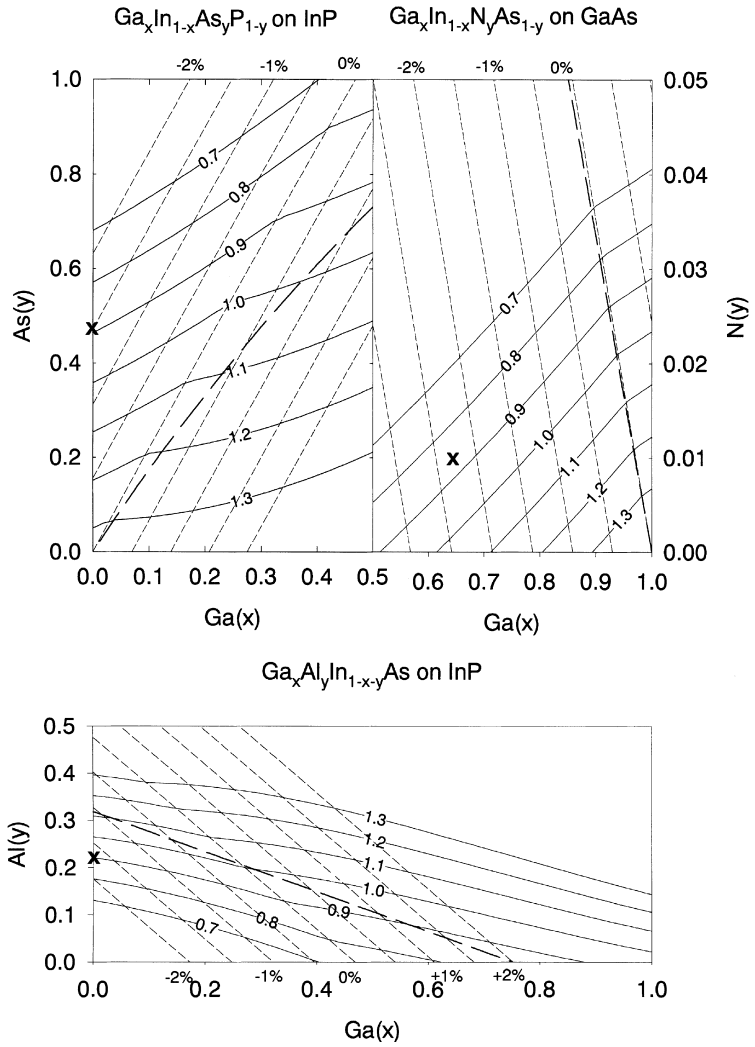

Fig. 1. Strain and strained bulk band gap energy versus material composition for GaInAsP, AlGaInAs and GaInNAs material systems.

Fig. 4 shows the gain spectra versus carrier density (from 1×10^{18} to 5×10^{18} cm^{-3}) for the above material systems. Only TE polarization gain spectra are shown for compressively strained quantum well systems. The peak gain versus injected carrier concentration is shown in Fig. 5. The gain spectrum for GaInNAs is shown without the correction factor, $f_{\Gamma c}$. If a factor of 0.8 were used (multiply the calculated result by 0.8) for GaInNAs, the peak material gain for the three systems is around the same. Here, we may have under-estimated the conduction band effective mass for GaInNAs as the

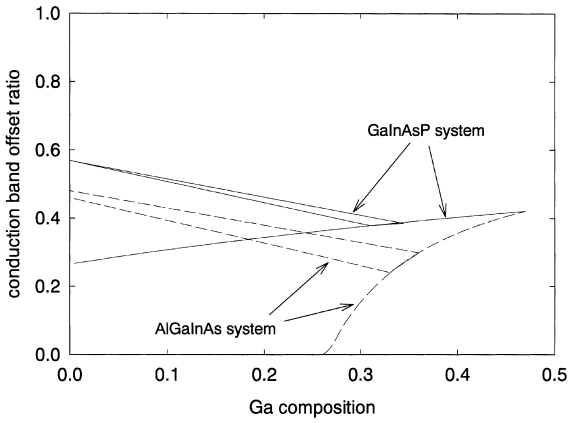

Fig. 2. Conduction band offset ratio versus Ga composition for lattice-matched and compressively strained GaInAsP and AlGaInAs systems on InP. The solid lines are for GaInAsP system, and the dashed lines are for AlGaInAs system.

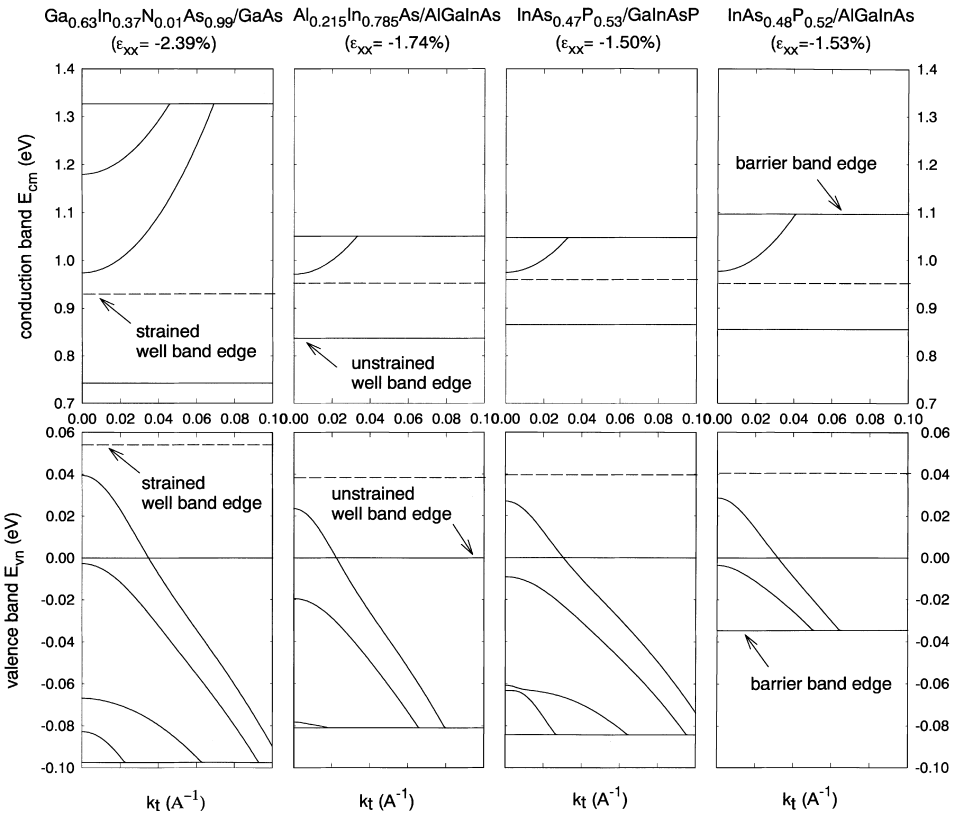

Fig. 3. Conduction and valence band structure for the four quantum well lasers. The solid horizontal lines are for unstrained well or barrier band-edges and the horizontal dashed lines are for strained well band-edges.

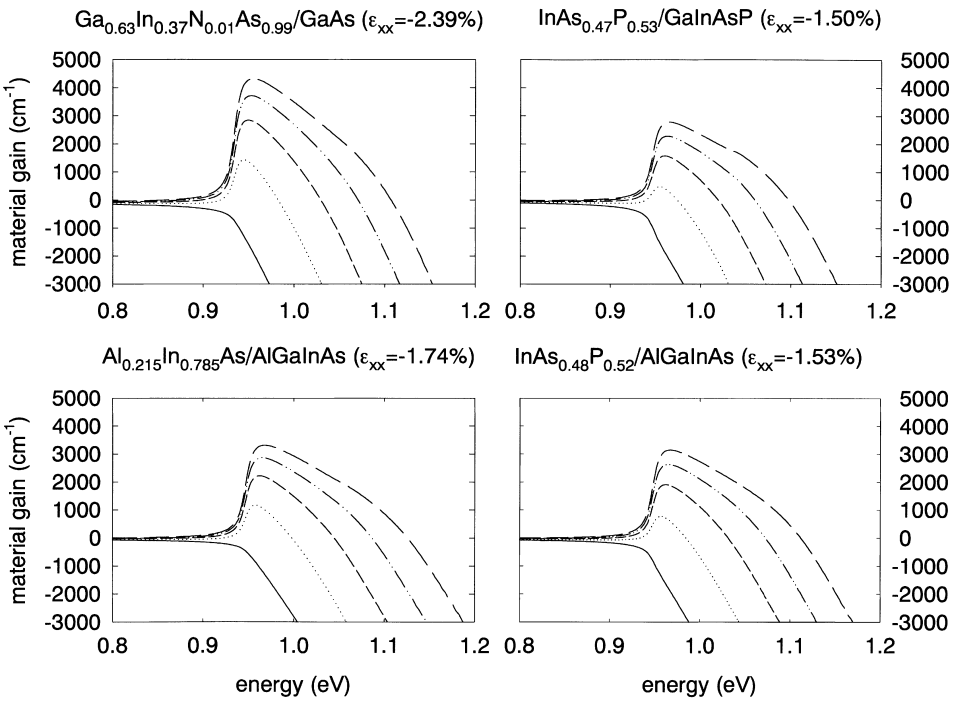

Fig. 4. Gain spectra versus injected carrier concentration for the four quantum well lasers. The injected carrier density increases from 1×10^{18} to 5×10^{18} cm^{-3}.

strong interaction from the N impurity may increase its value (Lindsay and O'Reilly 1999).

For the four material combinations considered here, the material gain is around the same, however, GaInNAs/GaAs outperforms the other in terms of conduction band offset. Its large band discontinuity as well as large conduction band offset ratio would contribute to superior high-temperature characteristics for temperature insensitive applications.

5. Conclusion

We have theoretically calculated the band structure and material gain for quantum well lasers of GaInAsP, AlGaInAs and GaInNAs systems emitting in 1300-nm band. The quaternary compositions are carefully chosen to maximize the conduction band offset of each material system. Four hetero-structure combinations out of three material systems are compared. Despite the differences in the band structure, the material gain is around the same for all these systems. However, the GaInNAs/GaAs system should be a better

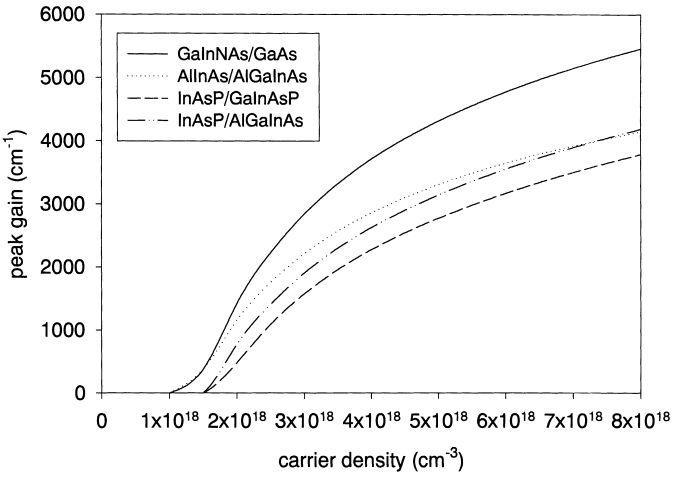

Fig. 5. Gain–carrier characteristics for the four quantum well lasers.

choice because of its large conduction band offset would decrease the carrier leakage over the barrier and the device's temperature sensitivity.

Acknowledgements

This work is supported by the National Science Council of the Republic of China under Contract NSC89-2218-E-009-055 and the LEE-MTI Foundation of the National Chiao Tung University.

References

Chuang, S.L. *Physics of Optoelectronic Devices*, John Wiley & Sons, New York, 1995.
Harrison, W.A. *J. Vac. Sci. Technol.* **14** 1016, 1977.
Kondow, M., T. Kitatani, S. Nakatsuka, M.C. Larson *et al. IEEE J. Select. Top. Quant. Electron.* **3** 719, 1997.
Lindsay, A. and E.P. O'Reilly. *Solid State Commun.* **112** 443, 1999.
Minch, J., S.H. Park, T. Keating and S.L. Chuang. *IEEE J. Quant. Electron.* **35** 771, 1999.
Takeuchi, K., T. Miyamoto, T. Kageyama, F. Koyama and K. Iga. *Jpn. J. Appl. Phys.* **37** 1603, 1998.
Van der Walle, C.G. *Phys. Rev. B. Phys.* **39** 1871, 1989.